

## Direct Observation of the Hot Electron Distribution Function in GaAs/AlGaAs Heterostructures

C. Wirner, C. Kiener, W. Boxleitner, M. Witzany, E. Gornik, P. Vogl, G. Böhm, and G. Weimann  
*Walter-Schottky-Institut, Technische Universität München, D-8046 Garching, Germany*  
 (Received 21 December 1992)

A new direct experimental technique to study the form of the hot electron distribution function is presented. Far infrared emission induced by a weak periodic potential is observed in high-mobility GaAs/AlGaAs heterostructures with extremely low electron density. The electric-field-dependent spectra give for the first time evidence of a nonequilibrium shape of the electronic distribution in the electric field direction. The onset of LO-phonon emission is clearly observed. Perpendicular to the applied electric field, a smooth form of the distribution is found. The results agree well with theoretical distribution functions obtained from the Boltzmann transport equation.

PACS numbers: 73.61.Ey, 73.40.Kp, 73.50.Fq

Extremely high mobilities in two-dimensional electron gases (2DEG) of GaAs/AlGaAs heterostructures give rise to new transport phenomena [1]. At low electric fields and low temperatures transport is dominated by electrons at the edge of the Fermi-Dirac distribution. Quantum effects and long ballistic mean free paths of several  $10\ \mu\text{m}$  are observed due to the effective suppression of impurity scattering [2]. With increasing applied electric field a rapid heating of the velocity distribution results in high electron drift velocities already at moderate external electric fields of  $\approx 10\ \text{V/cm}$  [3]. A gradual saturation of the average electron drift velocity to  $2 \times 10^7\ \text{cm/s}$  and a reduction of the mean free path to values varying from  $1\ \mu\text{m}$  to  $400\ \text{nm}$  is found at higher fields [4,5]. This has been attributed to the influence of LO-phonon emission as a dominant scattering mechanism in the hot electron regime [6,7]. Therefore the assumption of a quasiequilibrium hot Fermi gas is no longer valid and a nonequilibrium shape of the hot electron distribution function with a steep high energy tail is predicted. This situation might be evident in high-mobility single heterostructures with sufficiently low electron concentration where drift velocities are comparable or even higher than the Fermi velocity. To our knowledge no experimental analysis of the electric-field-dependent shape of the distribution function in such high-mobility GaAs/AlGaAs heterostructures has been reported so far.

This Letter presents a new experimental technique to analyze the electric-field-dependent shape of the heated two-dimensional distribution function in high-mobility GaAs/AlGaAs heterostructures. The drifting hot electrons are modulated by a weak periodic surface potential (inset Fig. 1). The potential acts as a coherent scattering source for the drifting carriers resulting in an energy loss via photon emission. This emission process is known in vacuum for relativistic electrons as the Smith-Purcell effect [8,9]. Observation of the effect in semiconductor structures is restricted to high-mobility samples with electron mean free paths exceeding the grating period length  $a$ .

The samples used consist of a  $2\text{--}6\ \mu\text{m}$  undoped GaAs

buffer layer grown on a semi-insulating GaAs substrate, a  $800\ \text{\AA}$  undoped  $\text{Al}_{0.41}\text{Ga}_{0.59}\text{As}$  spacer layer, a  $400\ \text{\AA}$   $\text{Al}_{0.41}\text{Ga}_{0.59}\text{As}$  Si-doped ( $15\ \delta$ -layers of  $n = 1.2 \times 10^{11}\ \text{cm}^{-2}$ ) layer, and a  $200\ \text{\AA}$  GaAs top layer. The depletion charge is  $n_{\text{depl}} = 0.6 \times 10^{11}\ \text{cm}^{-2}$ . The 2DEG formed in the undoped GaAs at the interface has an electron concentration of  $6 \times 10^{10}\ \text{cm}^{-2}$  and a mobility of  $\mu = 8 \times 10^5\ \text{cm}^2/\text{Vs}$ . A weak periodic potential modulation of the 2DEG is attained by periodically nanostructuring (grating period  $a = 200\ \text{nm}$ ) the GaAs top layer with a laser-holographic technique and shallow wet chemical etching which reduces the initial mobility only about 20%. The height of the weak periodic potential is determined to  $V_0 \approx 0.6\ \text{meV}$  at low electric fields by evaluating the additional magnetoresistance oscillations in the Shubnikov-de Haas effect [10].

The theoretically calculated intensity of the grating induced far infrared emission is determined in second order

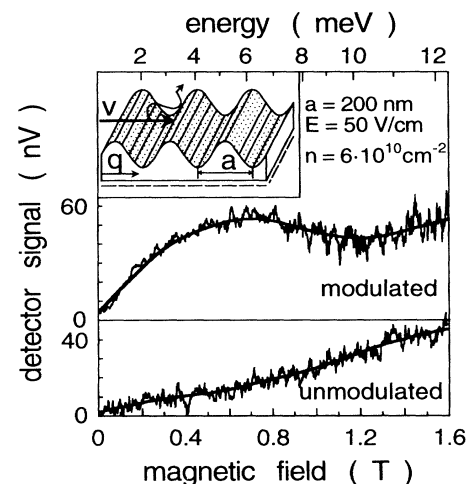


FIG. 1. Detector signal of radiation emitted from an unmodulated and a weakly modulated high-mobility GaAs/AlGaAs heterostructure at  $T = 4.2\ \text{K}$  and  $E = 50\ \text{V/cm}$ . Inset: Weak surface potential created by laser holography and wet chemical etching.

perturbation theory. For free electrons first order processes give no contribution to the radiation. The interacting potential consists of the weak periodic grating potential

$$V(x) = V_0 \cos(qx), \quad q = 2\pi/a, \quad (1)$$

and the electron-photon interaction potential

$$V(t) = \frac{e}{m^*} \sum_{\lambda} A_{\lambda} \mathbf{\epsilon}_{\lambda} e^{-i(\mathbf{K}_{\lambda} \cdot \mathbf{x} - \omega_{\lambda} t)} \cdot \mathbf{p}, \quad (2)$$

with  $A_{\lambda} = (\hbar/\epsilon\epsilon_0\omega_{\lambda}V)^{1/2}$  ( $V$  is the volume and  $\epsilon$  the relative dielectric constant).

Evaluating Fermi's "golden rule" and summing over all photon modes  $\lambda$ , the spectral power per unit area into the energy interval  $[\hbar\omega, \hbar\omega + d(\hbar\omega)]$  is

$$P(\omega) = \frac{e^2}{4\pi\hbar^2 m^* c^3 \epsilon\epsilon_0} |V_0|^2 \sum_{\pm q} \left\{ |q| \int dk_y f(\hat{k}_x(q, \omega), \hat{k}_y) [1 - f(\hat{k}_x(q, \omega) - q, \hat{k}_y)] \right\}, \quad (3a)$$

$$\hat{k}_x(q, \omega) = \frac{q}{2} + \frac{m^*}{\hbar q} \omega, \quad (3b)$$

where  $\hat{k}_x(q, \omega)$  is obtained by integration over the electron wave vector component  $k_x$  using the delta function for energy conservation [11]. The two-dimensional hot electron distribution function  $f(\mathbf{k})$  is obtained numerically by solving the Boltzmann integral equation [7]. In this calculation remote impurity scattering as well as LO-phonon emission and electron-electron interaction are taken into account. If the electronic distribution is sufficiently heated by the applied electric field and the electron density is small, only a few states are occupied and the electron gas is well described in a semiclassical picture [ $1 - f(\mathbf{k}) \approx 1$ ]. Then one can apply the semiclassical formula for the emission frequency  $\omega = \mathbf{v} \cdot \mathbf{q}$  ( $\mathbf{v}$  is the electron velocity and  $\mathbf{q}$  is the grating vector) derived from energy and momentum conservation rules. In this case the measured emission spectra can be interpreted as a direct picture of the semiclassical velocity distribution.

The experiments are performed in a liquid helium cryostat. The emitted far infrared radiation is guided to an optimized magnetic-field-tunable InSb cyclotron-resonance detector [12] via a light pipe. At 4.2 K the InSb detector has two absorption lines due to the impurity and the cyclotron resonance transition giving a resolution of  $\approx 1$  meV. The experimental setup is described in detail in Ref. [13]. Two emission geometries are used allowing current flow either parallel or perpendicular to the grating vector. In both cases only electrons with velocity components parallel to the grating vector make radiative transitions.

Figure 1 shows the InSb-detector response when an electric field of 50 V/cm is applied to the GaAs/AlGaAs heterostructure parallel to the grating vector. A broad structure develops in the periodically modulated structure sitting on a background emission which is also present in the unmodulated sample. The intensity of this background radiation increases slightly with the detector magnetic field. It is caused mainly by free carrier emission of the heated electron gas and has been investigated by Höpfel and Weimann [14]. The contribution of plasmon and intersubband emission to the observed emission signal can be excluded. Plasmon emission has been measured in a stronger modulated sample [15] with frequen-

cies independent of the electric field direction having a  $\sqrt{q}$  dependence contrary to the linear  $q$  dependence observed in the weakly modulated heterostructure. Intersubband radiation occurs at higher energies since the subband spacings are calculated for the present sample to be 19 meV [16,17].

In the further analysis the thermal background radiation (measured in the unmodulated sample) was subtracted to obtain the pure grating-induced far infrared emission in the modulated 2DEG. The detector magnetic field is converted to emission energy by calibrating the InSb detector with a magnetic-field-tuned, high-purity GaAs Landau emitter and a Fourier transform spectrometer. The impurity and the cyclotron resonance line shift nearly linearly with magnetic field. Note that the InSb detector becomes sensitive to far infrared radiation above a detector magnetic field of  $\approx 0.3$  T [12]. Consequently the analysis of the spectra is restricted to detector magnetic fields higher than 0.3 T.

Figure 2 displays the electric field dependence of the emitted radiation when the current is directed (a) parallel and (b) perpendicular to the grating vector. The uncertainty due to the noise and the resolution of the InSb detector is displayed by error bars. For an electric field of 37 V/cm a clear structure in the emission signal is observed. In the case of current parallel to the grating vector the increase of the external electric field results in a remarkable shift of the maximal emission signal to higher energies [Fig. 2(a)]. In addition the slope of the high energy decay becomes steeper at 75 V/cm. In the structure with current perpendicular to the grating vector [Fig. 2(b)] the maximum position of the signal is at lower energies and remains nearly unchanged with increasing applied electric field. Smooth decays of the high energy tail are found independent of the external field.

The samples are characterized by the average drift velocity and the mobility (Fig. 3) determined from transport measurements. A gradual saturation of the drift velocity and a mobility loss is found with increasing external electric field. The electric field values investigated by far infrared emission are indicated in Fig. 3 as arrows.

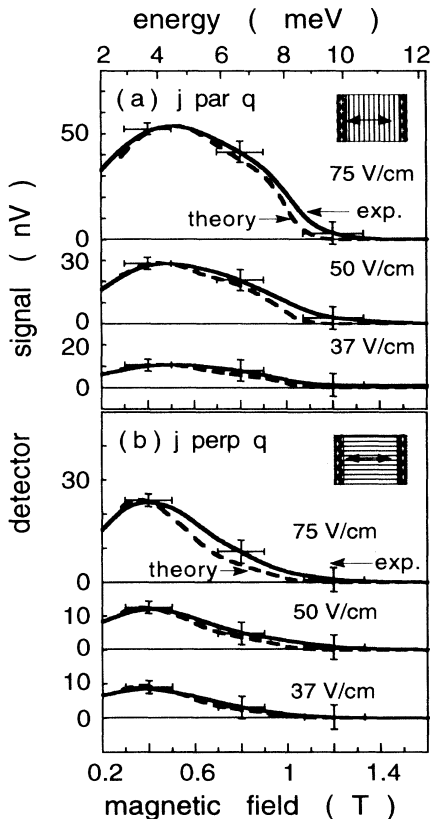


FIG. 2. Detector signal of grating-induced far infrared emission with current parallel (a) and perpendicular (b) to the grating vector as a function of applied electric field (solid lines). Theoretical emission spectrum from a distribution function calculated by numerically solving the Boltzmann transport equation after formula (3a) (broken lines).

It is remarkable that the energy position of the high energy tail of the emission spectrum at 75 V/cm in Fig. 2(a) corresponds to the electron momentum at the LO-phonon energy according to  $\omega = \mathbf{v} \cdot \mathbf{q}$ . At the same electric field the average drift velocity derived from transport measurements starts to saturate (Fig. 3) which is attributed to the onset of LO-phonon emission.

The experimental spectra are compared with a calculation of emission spectra as described by Eq. (3a). Figure 4 shows the intersection lines of electric-field-dependent two-dimensional distribution function used in Eq. (3a) parallel (a) and perpendicular (b) to the field direction. A pronounced momentum shift of the distribution caused by the electric field can be seen in drift direction. With increasing applied electric field the maximum of the distribution shifts to higher  $k$  values. The onset of LO-photon emission leads to a steep decay of the distribution function. As a result of the small electron density of  $6 \times 10^{10} \text{ cm}^{-2}$  electron-electron interaction is too weak to thermalize the LO-phonon-induced cutoff sufficiently. Consequently the high energy tail deviates from a heated

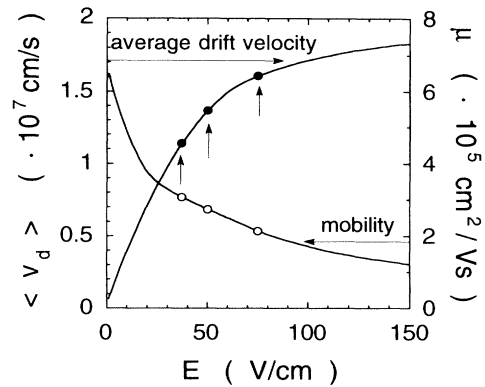


FIG. 3. Electric field dependence of average drift velocity and electron mobility derived from current-voltage measurements. The arrows mark electric fields where the far infrared emission signal is recorded.

Fermi-Dirac distribution. Note that the occupation number of the maximum of the distribution function is about 0.2 due to the small electron density and the high mobility of the sample. Consequently the observed spectra are really related to the distribution function as the condition  $[1 - f(\mathbf{k}) \approx 1]$  is fulfilled. The grating-induced far infrared emission spectra of the calculated distribution functions of Figs. 4(a) and 4(b) are displayed respectively in Figs. 2(a) and 2(b) as broken lines. The InSb detector characteristic is taken into account by weighting the spectra with the magnetic-field-dependent InSb-detector responsivity [12]. A good agreement between theory and the experimental data is found. All characteristics of the theoretical distribution function are clearly reflected in the emission spectrum.

Experimental results in Fig. 2(a) (current parallel to

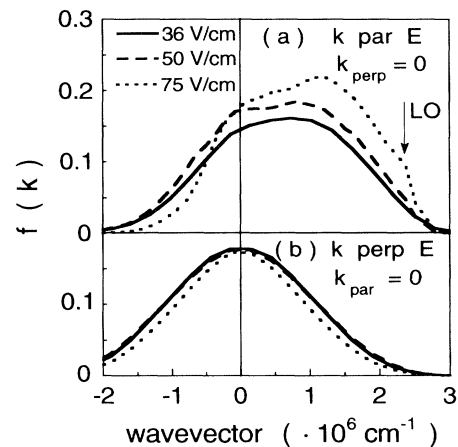


FIG. 4. Intersection lines of the two-dimensional theoretical distribution function determined from the Boltzmann-transport equation (a) parallel and (b) perpendicular to the electric field at three different external electric fields.

grating vector) are related to the intersection of the distribution function in drift direction. As long as LO-phonon emission is weak the only effect of the applied electric field is a momentum shift and a heating of the initially cold Fermi-Dirac distribution. At higher external fields the experiments show for the first time a remarkable transition to a nonequilibrium distribution due to LO-phonon emission. In this electric field regime the simple electron temperature model cannot be applied to describe the hot electron distribution function of high-mobility GaAs/AlGaAs heterostructures with low electron densities. Therefore we conclude that a nonequilibrium shape is present in high-mobility and *very*-low-density structures. LO-phonon emission then becomes the dominant energy relaxation mechanism whereas electron-electron interaction is weak.

The experimental results in Fig. 2(b) (current perpendicular to grating vector) are related to the intersection of the distribution function perpendicular to the electric field. The experiments show that the shape of the emission spectra has a smooth decay at higher energies contrary to the results of Fig. 2(a). This effect is confirmed by the symmetric and smooth shape of the theoretically calculated distribution function depicted in Fig. 4(b). The smooth decays are caused by scattering events resulting in a heating of the initially cold Fermi-Dirac distribution perpendicular to the drift direction. The experimentally observed differences in the emission spectra parallel and perpendicular to the grating vector are due to the small Fermi energy in the low-electron-density sample. Electron-electron interaction is too weak to generate similar shapes of the distribution parallel and perpendicular to the applied electric field.

In conclusion, we have measured far infrared radiation emitted from periodically nanostructured high-mobility GaAs/AlGaAs heterostructures. This Smith-Purcell type radiation provides a new experimental technique to investigate the electric-field-dependent heating of the hot electron distribution function in high-mobility single heterostructures. When the electric field is directed parallel to the grating vector the shape of the distribution function in drift direction is observed. The experimental results show for the first time a significant change of the distribution function from a quasiequilibrium heated Fermi-Dirac distribution to a nonequilibrium distribution developing a steep high energy tail at the LO-phonon energy. Perpendicular to the applied electric field the spectra are remarkably different having smooth high energy tails at lower energies which is attributed to the small Fermi en-

ergy in the low-electron-density sample. The Smith-Purcell-type emission is only observed in very-high-mobility samples. If the sample mobility is strongly reduced by deeper etching the emission spectra do not depend on the electric field direction. Theoretical distribution functions obtained from the Boltzmann transport equation are in good agreement with the experimental data clarifying the importance of LO-phonon emission as the dominant energy relaxation mechanism in high-mobility heterostructures. This results in an asymmetric velocity distribution present at high electric fields.

The authors are grateful to K. Bochter for optimizing the InSb detector and G. Zandler for valuable discussions. This work was sponsored by the Deutsche Forschungsgemeinschaft.

- 
- [1] K. Hirakawa and H. Sakaki, Phys. Rev. B **33**, 8291 (1986).
  - [2] H. van Houten, B. J. van Wees, J. E. Mooij, C. W. J. Beenakker, J. G. Williamson, and C. T. Foxon, Europhys. Lett. **5**, 721 (1988).
  - [3] K. Hirakawa and H. Sakaki, J. Appl. Phys. **63**, 803 (1988).
  - [4] W. T. Masselink, N. Braslau, D. LaTulipe, W. I. Wang, and S. L. Wright, Solid State Electron. **31**, 337 (1988).
  - [5] A. Palevski, M. Heiblum, C. P. Umbach, C. M. Knoedler, A. N. Broers, and R. H. Koch, Phys. Rev. Lett. **62**, 1776 (1989).
  - [6] X. L. Lei and C. S. Ting, Phys. Rev. B **32**, 1112 (1985).
  - [7] C. Kiener and E. Vass, J. Appl. Phys. **64**, 6365 (1988).
  - [8] S. J. Smith and E. M. Purcell, Phys. Rev. **92**, 1069 (1953).
  - [9] G. Doucas, J. H. Mulvey, M. Omori, J. Walsh, and M. F. Kimmitt, Phys. Rev. Lett. **69**, 1761 (1992).
  - [10] R. R. Gerhardt, D. Weiss, and K. v. Klitzing, Phys. Rev. Lett. **62**, 1173 (1989).
  - [11] C. Kiener, W. Boxleitner, C. Wirner, and E. Gornik (to be published).
  - [12] G. Strasser, K. Bochter, M. Witzany, and E. Gornik, Infrared Phys. **32**, 439 (1991).
  - [13] E. Gornik, W. Müller, and F. Kohl, IEEE Trans. Microwave **22**, 12 (1974); **22**, 991 (1974).
  - [14] R. A. Höpfel and G. Weimann, Appl. Phys. Lett. **46**, 291 (1985).
  - [15] R. A. Höpfel, G. Lindemann, E. Gornik, G. Stangl, A. C. Gossard, and W. Wiegmann, Surf. Sci. **113**, 118 (1982).
  - [16] E. Gornik and D. C. Tsui, Phys. Rev. Lett. **37**, 1425 (1976).
  - [17] M. Helm, P. England, E. Colas, F. DeRosa, and S. J. Allen, Jr., Phys. Rev. Lett. **63**, 74 (1989).